Contact Conditions over Turnout Crossing Noses

Contact Conditions over Turnout Crossing Noses

Mehmet Zahid Hamarat [1], Sakdirat Kaewunruen [1], Mayorkinos Papaelias [2]

[1] Birmingham Centre for Railway Research and Education, Gisbert Kapp Building, The University of Birmingham, B15 2TT, United Kingdom
[2] School of Metallurgy and Materials, The University of Birmingham, B15 2TT, United Kingdom

mzh670@bham.ac.uk

Abstract. Even though railway systems are becoming a more preferred transportation concept regarding high speeds, punctuality, safety, availability, which are appealing for passengers; cost-effectiveness, environmentally friendliness and less soil occupation corresponding to other transportation modes, which attracts the governments and operators, it still suffers from two major drawbacks: first investment and high maintenance costs. Life cycle costs analyses show that maintenance costs have significant effects on the total value as well as early investment costs. The reason for high maintenance costs in railway systems is that critical components (i.e. turnouts), which are the weak points of a railway system, require frequent detailed inspection and maintenance associated with high safety standards. For instance, it is widely known for a turnout that European countries have conducted a series of projects such as Innotrack, IN2Rail, S-code in order to lower the maintenance costs. Moreover, turnouts also restrict the design limits of a railway system, which results in lower operational speeds. Consequently, studies on turnouts have been increasing. In general, the studies focus on track stiffness along the turnout, environmental effects on configuration, conversion problems and the contact problem. Among these issues, the issue regarding contact is the most premature problem due to its nonlinear nature, which could not be solved analytically. Having increased computational power, sophisticated methods for the contact problem have been developed. The problem regarding the contact patch, forces and positions are of considerable interest. From the aspect of turnout crossing noses, there is a contact patch evolution on crossings from single to double and double to single contact patch, which affects the vehicle dynamics to a large extent. Numerous studies have been presented for the problem. However, these studies, commonly, consider one type of turnout, mostly standard turnouts. Regarding the absence of collective study, in this study, the aim is to review the contact conditions depending on turnout types from a wider perspective. As result of the study, it has been found that crossing nose types such as fixed and movable have significant effects on lateral and vertical movements of the contact patches. Moreover, different layouts of turnouts have different effects on the contact conditions.

1. Introduction

Rail-wheel interface or contact is a major problem which needs to be solved in the field of railways [1]. Due to the complex nature of contact, analytical solutions are restricted. Having been increased computational power, the numerical studies on the contact have been providing a better understanding. As a result, the other problems (i.e. deformations on turnout crossings) associated with the contact have simultaneously been investigated. Turnouts providing flexibility in railway operations by enabling to change the direction of the railway vehicle from one route to another route are critical components as

they restrict the operational speed and cause complicated wheel dynamics. Therefore, different turnout configurations have been in use depending on the speed or layout such as gauge widening[2], undercut switch blades [3], movable crossings [4] and so on. A typical turnout consists of three sections: switch, closure and crossing panels. At closure panel, the wheel-rail dynamics show a similarity to normal track dynamics, which is generally a single contact problem. On the other hand, switch and crossing panels present a different behaviour called two-contact problem. At crossings, this two-contact problem causes high impact forces resulting in plastic deformation and fracture [5, 6], which attracts the researchers. As a result, there have been many experimental and numerical studies on turnout crossings. Experimental studies usually consider the loads and wheelset positions regarding track stiffness, turnout direction, routes and speeds. Numerical studies also cover the same properties but additionally contact patch area, contact forces and contact positions. The numerical studies could be based on Finite Element Analysis or Multibody Simulation. The difference between both methods is the accuracy of contact patch properties and calculation time [7, 8].

The current paper begins by reviewing contact properties of the fixed common crossing nose commonly used in turnout studies. Then, studies on the diamond or obtuse crossings are presented. Finally, contact properties of the movable crossing nose are demonstrated.

2. Contact Properties of Crossings

2.1. Fixed Crossings

In railway tracks, fixed crossings are widely used up to 200 km/h for normal and medium axle loads. For higher speeds, movable crossings must be used [4]. Fixed crossings could practically be categorized as common crossings and diamond crossings.

2.1.1. Common crossings. At a common crossing, as can be seen from **Figure 1**, there is a discontinuity in the area of crossing nose. This discontinuity affects the contact properties significantly (i.e. vertical contact forces, contact patch area and position, …). Under ideal conditions, the rolling motion of the wheel from wing rails to the crossing nose is assumed to have a smooth motion. The magnitude of the impact force is expected to be small, estimated at maximum 30-50 percentage of the static wheel-rail contact force [9]. However, for uneven transition, the severity of contact forces and the position of contact patch depends on strongly track properties and vehicle parameters. Likewise, determining the contact properties depends on methodology (i.e. field experiments or numerical analysis) and the capability of the numerical tools.

Figure 1. A standard turnout crossing nose [6]

In an early study, probably the first, Andersson was built a Multibody Simulation (MBS) model adjusted with the outputs of Finite Element(FE) model of UIC60-760-1:15 standard turnout to investigate crossing nose contact properties. The model was called "Linear Track" where the rail pads and ballast were considered linear springs (former 140MN/m and latter 150 MN/m) and the modal damping (45 kNm/s and 180 kNs) was applied. Contact problem was solved with Non-Hertzian contact theory and Coulomb's friction theory. The axle load of the vehicle moving in through route of facing direction was 150 kN [9]. Even though the model is a preliminary model, it captured good results (**Figure *2*** and **Figure *3***).

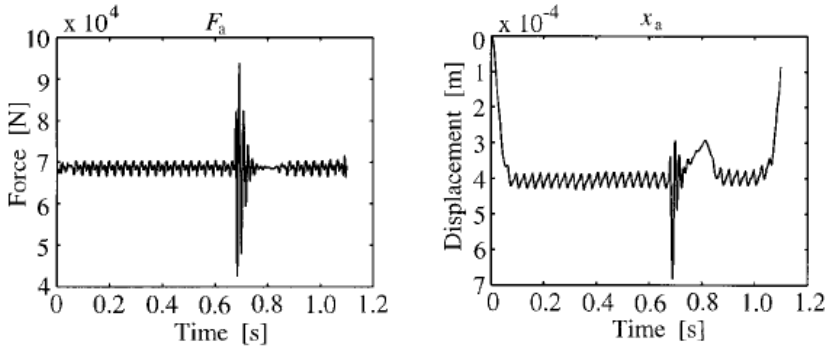

Figure 2. Vertical forces (left) and vertical displacements (right) [9]

In Figure 2, it was assumed that the motion is smooth. Nevertheless, a vertical contact force emerged as a result of the discontinuity in the track stiffness. Moreover, after the impact force, wheel displacement decreases, meaning that contact patch area becomes zero with respect to the stable wheel position. In **Figure *3***, roughly, the effect of irregularity and vehicle speed is presented. As can be seen from the figure, higher amplitude irregularities or speeds could cause higher or lower contact forces. However, it is not clear when the maximum or minimum forces occur. Therefore, the model provides an elementary knowledge of the contact properties in the through route of facing direction regarding vehicle speeds and the discontinuity at crossing nose.

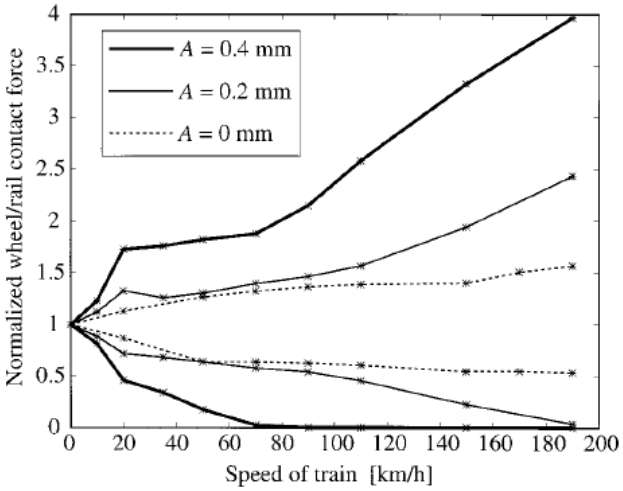

Figure 3. The effects of crossing irregularities on the vertical wheel force [9]

An improved model is offered by [10] in which the same method [9] is used for the solution. The difference is that the range of modal superposition method was increased up to 500 modes. Thus, it is assumed that the result of vertical contact forces and vertical displacement of the wheels are more accurate as regards the variations in parameters of both models. The model also includes the dynamics

of the vehicle in the diverging route of facing direction, which reflects the effect of discontinuity at crossing nose on the lateral displacement of the wheel (related to lateral contact patch position) and lateral forces acting on the contact patch (Figure 4). However, Kassa points out that the model is still insufficient to represent the crossing phenomenon due to the limitation in modes number selection related to computational cost [10]. For this purpose, a new method, Green's function, to effectively solve the differential equations in MBS model is offered. It was believed that this method is consistent with the solutions of classical MBS model and fast when it is compared with classical MBS models. Furthermore, it offers a more detailed representation of the turnouts, which gives more distinct results of contact patches. [7]

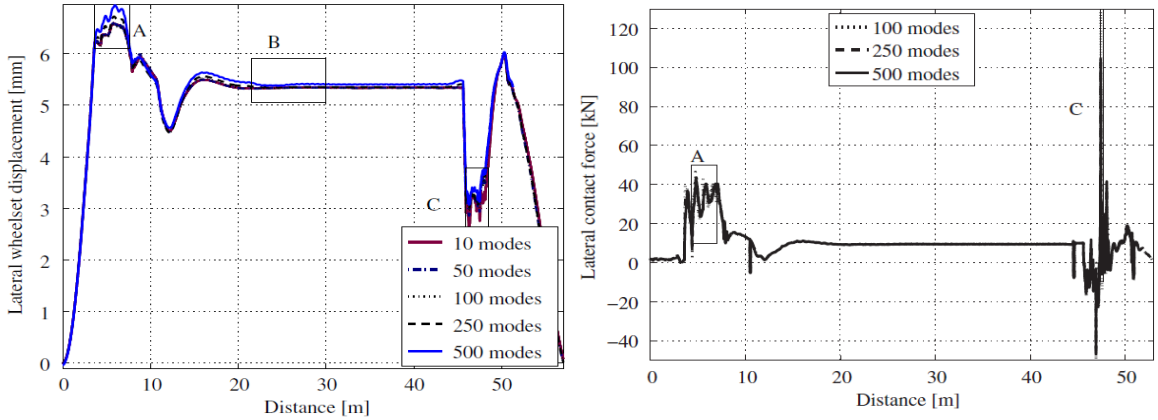

Figure 4. Lateral wheel displacements and forces at turnouts [10]

There exist numerous research using MBS to determine contact properties of vehicle-crossing nose interaction under different conditions [11-13]. For instance, the direction and route have a great influence on contact. Moving direction affects significantly the lateral contact forces as well as route. It is highest in the facing-diverging state. Nonetheless, vertical contact forces are not influenced by facing or trailing move but affected by diverging or through routes. The diverging causes higher vertical contact forces [14]. As well known, the wheel-rail interaction is a complicated problem as the wheel and rail profiles changes in time which affects the contact properties significantly at crossing nose as well as the normal track. In Figure 5, this effect is well presented where 120-wheel profiles are induced to 20-wheel profiles by stochastic approaches. Here, it should be emphasized that after closure panel, check rails prevent the wheels hitting the crossing nose when the rolling radius of the wheel on the crossing nose side decreases and the steering movement occurs at approximately 45m.

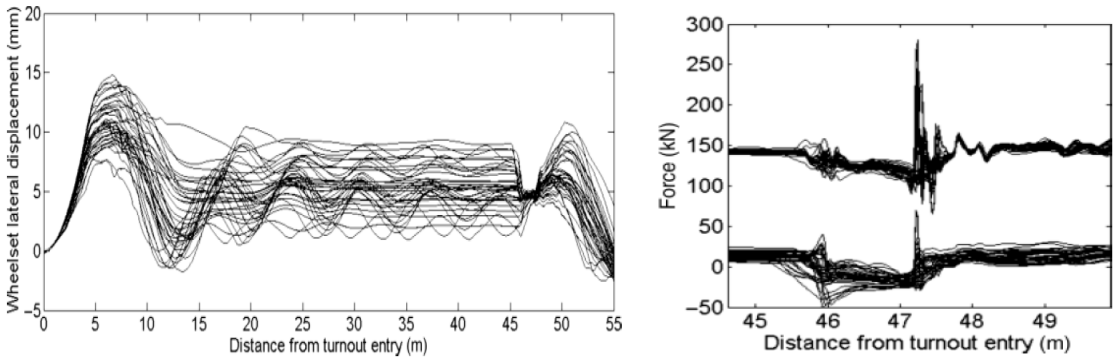

Figure 5. Lateral wheel displacements (left), vertical forces (right-top lines) and lateral forces(right-bottom lines) [15]

Contact properties even depend on the types of profile change [15, 16]. For instance, if the profile change is in the form of hollow wear, the vehicle acts differently in crossing panel owing to the false

flange (Figure 6). The wheel climbs up to pass over the false flange and falls on the crossing nose, causing higher impact forces and wider contact patch area.

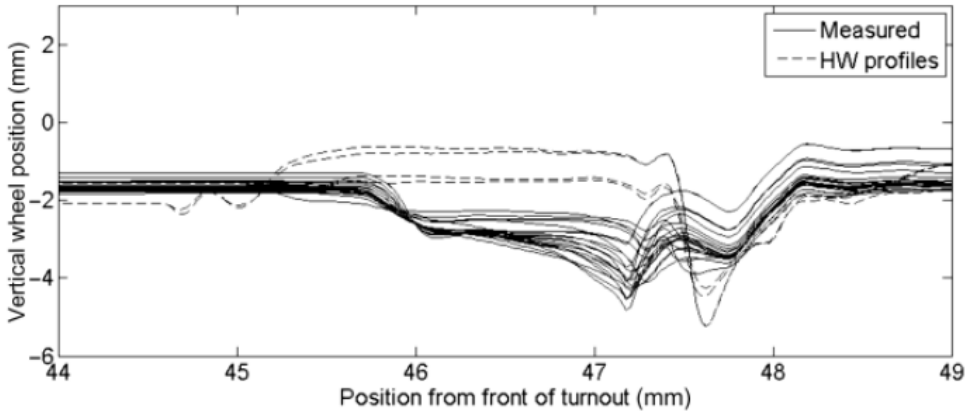

Figure 6. Force variations depending on the wear type [15]

Changes in the crossing nose profile (i.e. wing rail-crossing difference, crossing nose transverse rail profile, crossing nose vertical profile) also influence the contact properties [17]. In Figure 7, the vertical nose profile is modified based on the variation in the height of the specific two design points. "h=0" represents original nose profile and the others indicate raised or reduced profile height. As can be seen from the figure, increasing the profile height reduces the vertical and lateral displacement. On the other hand, it increases the vertical contact forces.

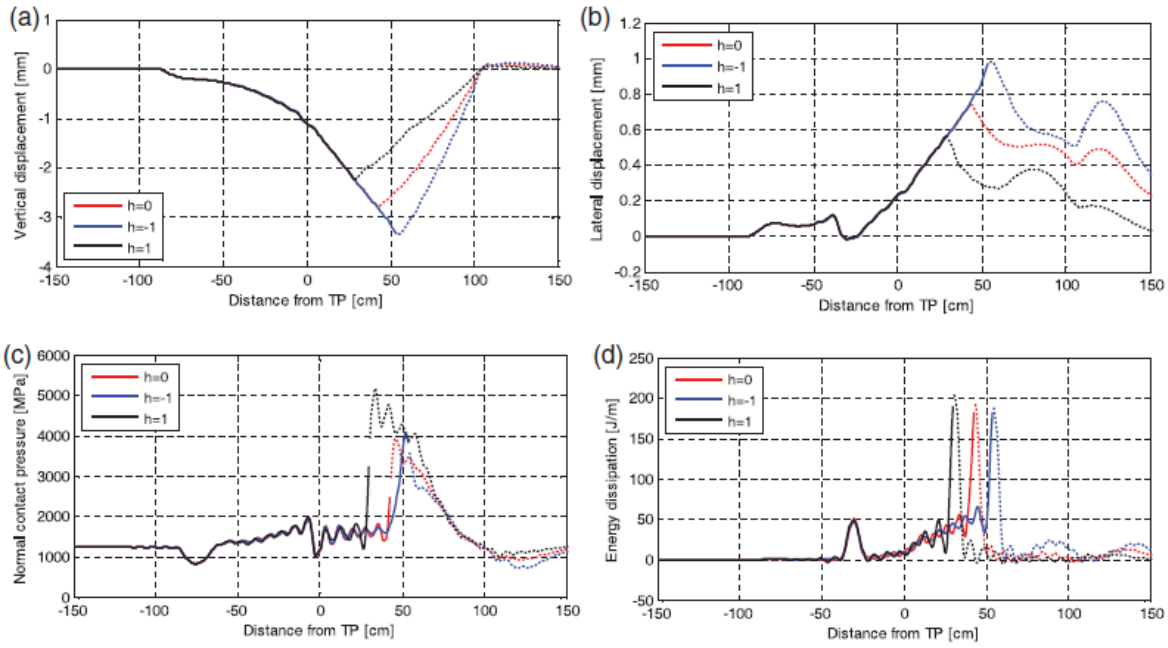

Figure 7. Contact properties at crossing nose depending on the rail profile variations [17]

Modelling in MBS environment could be fast and practical; however, they suffer from several drawbacks while investigating the contact position on crossing nose. The first problem is that MBS programme could be insufficient to calculate the high-frequency excitations such as rail irregularities

with wavelength 1-10 cm where excitation value is bigger than 1kHz [18]. Specifically, the impact forces acting on crossing nose is higher than 200 kHz. [2] Therefore, the selection of proper MBS programme is also vital to define the contact properties accurately. Another disadvantage is that the contact properties (positions, area, forces) depend also contact theories used in the simulations. For instance, in Figure 8, the contact areas of different theories are compared. From left to right, the accuracy of contact properties increases. As a result, the popularity of FE models has been increased.

FE methods define the contact patch behaviours of the bodies in contact with high accuracy regarding the three-dimensional geometries of the bodies and do not require any assumptions to simplify the contact properties [19]. Moreover, FE is an effective method to solve the elastic-plastic contact problems, for instance, in contrast to Hertzian contact where the half-body assumption is required. Additionally, plastic deformations of the contact patch or strain level investigations are only possible in FE environment [8]. Therefore, FE has become a powerful numerical tool to study the contact conditions at crossing nose.

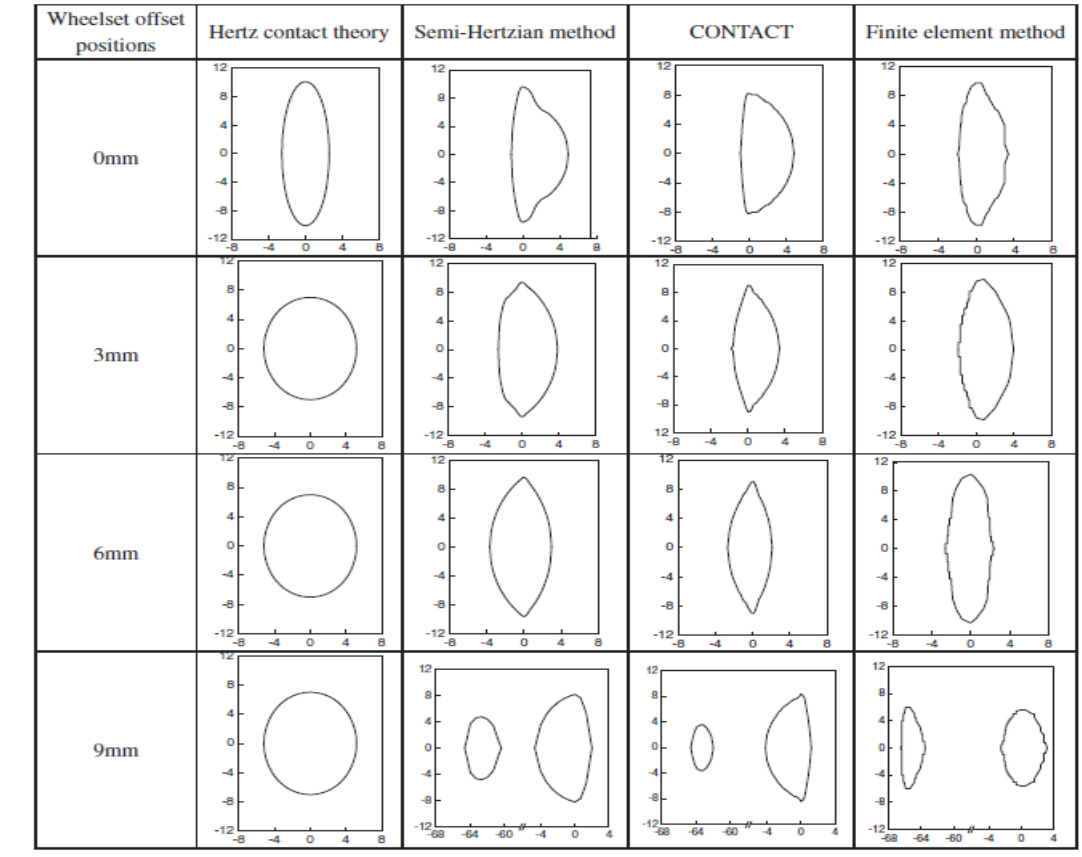

Figure 8. Contact patch areas regarding different contact theories [20]

On the other hand, effectiveness and efficiency of the FE model are related to FE programmes and computational power. For instance, due to lack of computation power [21], prior models should have been simplified [22]. However, the simple FE model is also adequate to provide a better understanding of contact properties on the crossing such as the effects of the speed, the nose geometry and the wheel lift where the contact patch area is zero. For instance, the dynamic factor of FE model is between 2.5 to 3.8 depending on the velocities [23]. Moreover, these models could be adapted to different damage models based on strain-stress level. Nevertheless, early models do not account for the slippage of the contact patches. Interestingly, parallel to advances in computers, more detailed FE models have been built. First, three-dimensional FE model including slippage, the whole structure of turnout and wheel

was modelled. [21]. Later, the model is used for different axle-loads and materials ranging from elastic to elastic-plastic [24]. The model was qualitatively consistent with MBS models, as the inputs of the models vary. Nonetheless, the model applied several boundary conditions (i.e. no lateral movement of the wheel, no yaw motion, …) to reduce the computational power, which results in loss of accuracy to determine contact patches.

A more advanced model was proposed by [8], where a wheelset and the turnout were modelled. Hence, there are no limitations on wheelset movements through the crossing nose, which provides realistic results [25]. However, the model did not account for the slippage on the contact patches. Therefore, another model capable of presenting slippages and shear forces on the contact patch[26] was established and validated with field measurements (Figure 9).

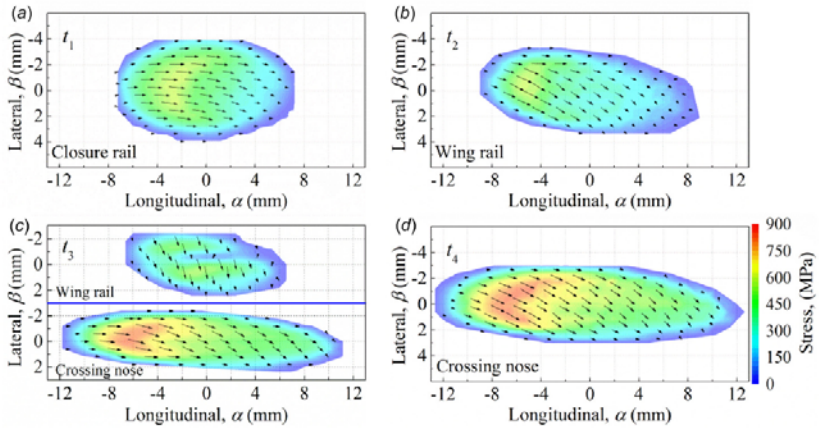

Figure 9. Shear forces on the contact patches [26]

The more details in the FE model demands the more computational power. Nevertheless, the demand and the technological advance in computers is not parallel. Therefore, a need to reduce computational demand for FE model emerged. Ma suggested a solution where the FE model is enhanced with another software searching potential contact areas to reduce the computational cost by tuning the mesh elements size around the potential contact areas and the rest of the model [27]. The result of this approach is presented in Figure 10 and Table 1. As can be seen from the figure, contact patch area becoming smaller towards the crossing nose reaches the highest value after the completed transition. However, the highest contact force (616 kN) occurs during the transition at section D. Further, considering the contact patches and pressures, contact force fluctuates for a while after the transition. Apart from these, the contact patch shifts in the outward lateral direction through the transition point and then, the inward lateral direction after the transition point, inherently. Even though vertical displacements are not presented in this paper, they are validated with field experiments [27].

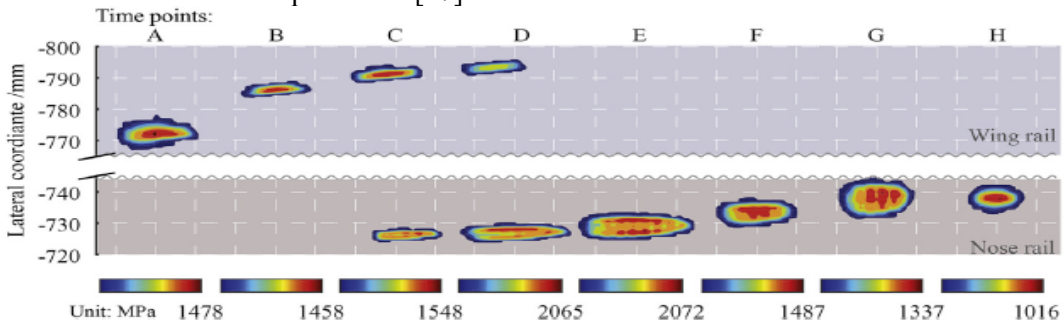

Figure 10. Contact patches during the transition over the crossing nose [27]

Table 1. Figure 10 in numbers [27]

	W/C impact at different time points							
	A	B	C	D	E	F	G	H
Contact status[a]	1	1	2	2	1	1	1	1
σ_n^{max}/MPa[b]	1478	1458	1548	2065	2072	1487	1337	1016
τ^{max}/MPa[c]	326	423	460	542	451	279	262	278
A_c/mm^2[d]	156.2	64.8	154.3	298.5	215.2	154.8	202.0	105.0

[a] Number of contact patches.
[b] Maximum normal pressure.
[c] Maximum shear stress.
[d] Area of contact patch.

2.1.2. Diamond or Obtuse Crossings. Diamond crossings may be the second most common crossing type in railway tracks [28]. Nonetheless, the numerical studies considering the contact behaviour of this type are rare. In 2006, Xhu investigated contact properties of a diamond crossing with a new contact algorithm in NUCARS[1]. The results only reflect the contact forces. Regarding the common crossings, one can conclude that the results are qualitatively consistent since the details of the simulation are not clear (**Figure 11**). Moreover, the diamond crossing used in the simulation is a special kind of diamond crossing, namely one-way-low-speed diamond crossing.

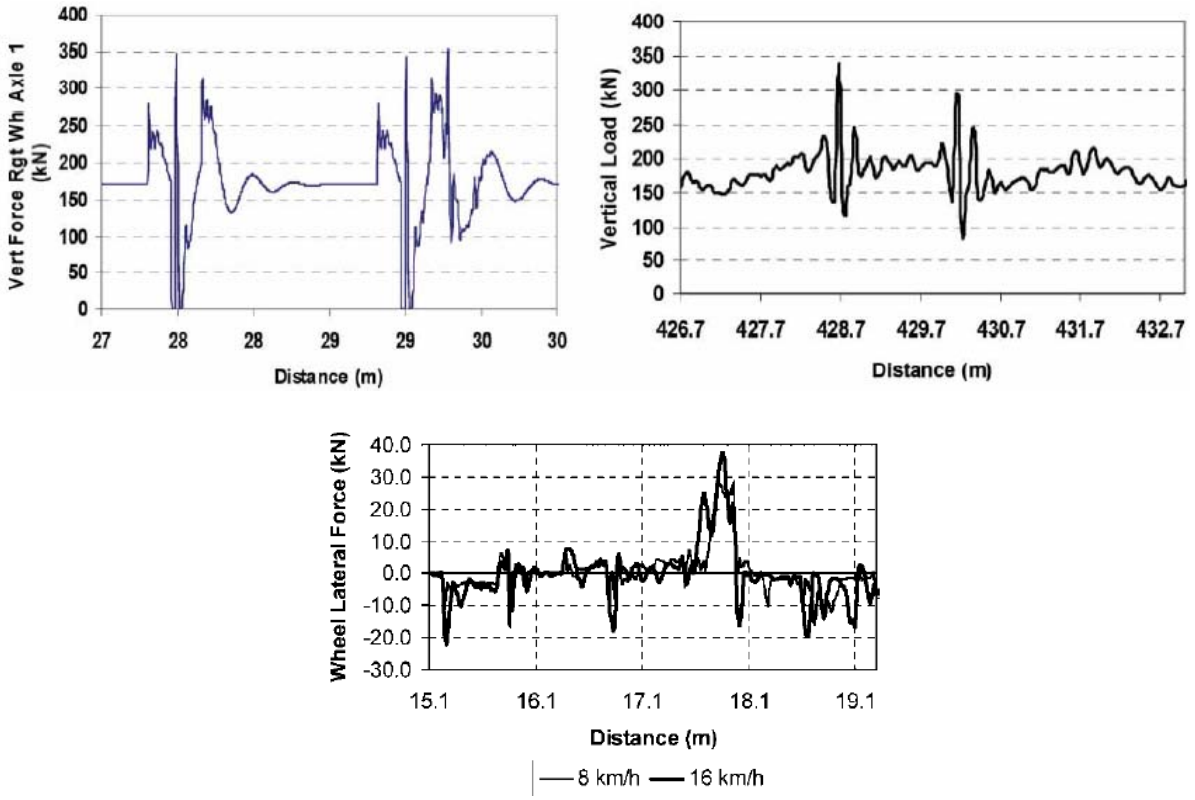

Figure 11. Vertical forces - numerical (left-top) and experimental (right top) and numerical lateral forces (bottom) at diamond crossings [1]

In Figure 11, the magnitude of impact force seems approximately two times higher than the static loading. The two picks in the graphic are due to passing over two discontinuities in the crossing panel. Lastly, as can be seen from the figure, the discontinuity also results in a lateral impact force even at low speeds.

2.2. Movable Crossings

The discontinuity in fixed crossing causing high impact forces disappears in movable crossings. (Figure 12) Therefore, movable crossings are used for the vehicle speed over 200 km/h [4]. Nonetheless, there still appear to occur impact forces on crossing point(nose). This is likely to be related to the flexibility of the point rail (crossing nose) and track stiffness [20, 29].

Figure 12. A typical movable crossing [30]

Contact behaviour seems to be similar to fixed nose crossing. During the transition, there is the load transition between point rail and stock rail of crossing side as a result of two contact problem [20]. In Figure 13, the transition effect could be seen. Contact point first moves outward while the wheel moves one rail to another rail and then, after load transition, it jumps the other rail and moves inward while the wheel becomes distant to crossing nose. Hence, it could be assumed that the factors affecting on contact properties of fixed turnouts also influence the movable crossings (i.e. rail or wheel profile[31], wheel diameter[32], direction or route [31], etc.).

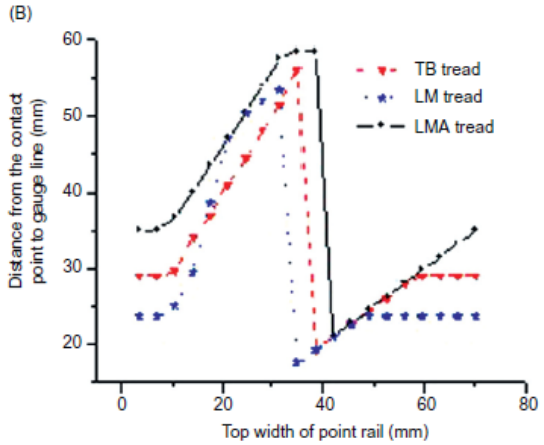

Figure 13. The contact patch positions on the crossing rails [31]

The advantage of movable crossing, maybe the only difference depending on the present knowledge, it reduces the impact forces and displacements well [33]. As can be seen from Figure 14, displacements and forces decreased considerably.

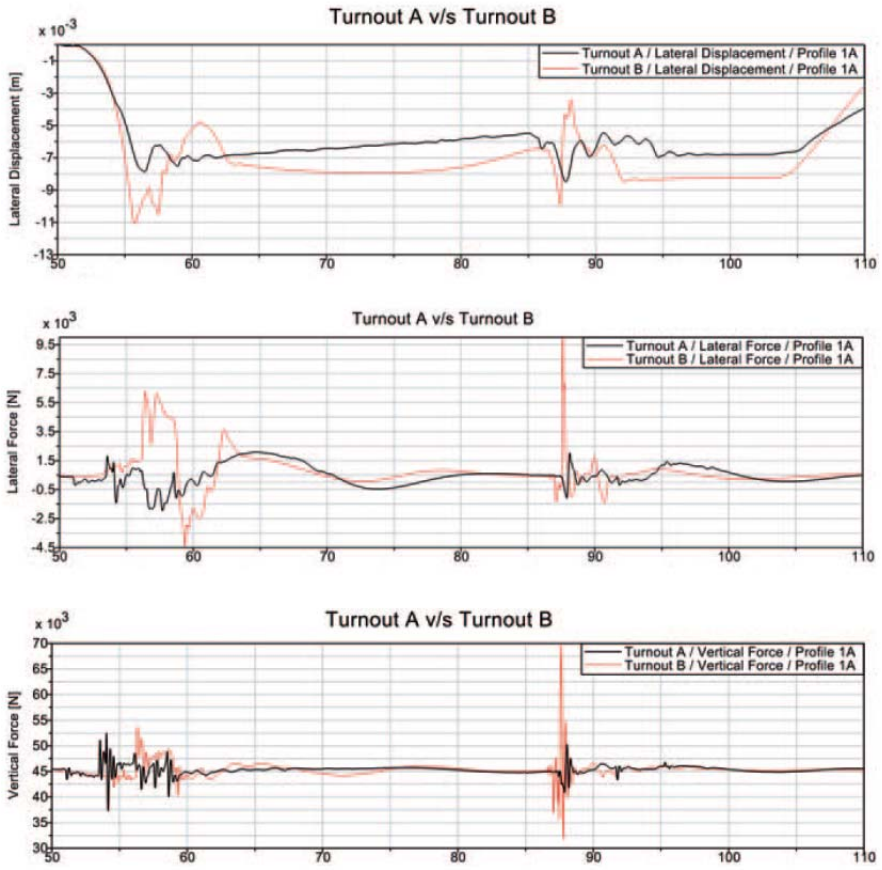

Figure 14. Comparison of common and movable crossings [33]

3. Conclusions

This review has considered the issues surrounding contact properties. Parallel to computational technology, the number of studies has been increasing. Latest studies prefer FE method to be more accurate to determine contact properties. However, the studies are still scarce regarding the contact nature. Therefore, more studies are required to make certain comments. Depending on this study, it could be concluded that crossing nose types (i.e. fixed or movable) have different effects on lateral and vertical movements of the contact patches. Moreover, layout type could influence contact properties.

Acknowledgment(s)

The first author would like to express his gratitude to the Ministry of National Education (MEB) and ITU for the scholarship. The authors sincerely appreciate the European Commission for the project H2020- "RISEN: Rail Infrastructure Systems Engineering Network", which provides a global research environment, www.risen2rail.eu.

References

[1] X. Shu, N. Wilson, C. Sasaoka, and J. Elkins, "Development of a real-time wheel/rail contact model in NUCARS®1and application to diamond crossing and turnout design simulations," *Vehicle System Dynamics,* vol. 44, pp. 251-260, 2006.

[2] B. A. Pålsson, "Optimisation of Railway Switches and Crossings," Department of Applied Mechanics, Chalmers University of Technology, Gothenburg, 2014.

[3] *National Rail Turnouts Workshop*, Brisbane, 2014.

[4] C. Esveld, *Modern railway track*, Delft: Technische Universiteit, Delft, 2001.

[5] N. Burgelman, "The Wheel-Rail Contact Problem in Vehicle Dynamic Simulation," TU Delft, Delft, 2016.
[6] S. Kaewunruen, "Monitoring structural deterioration of railway turnout systems via dynamic wheel/rail interaction," *Case Studies in Nondestructive Testing and Evaluation,* vol. 1, pp. 19-24, 2014.
[7] X. Li, P. T. Torstensson, and J. C. O. Nielsen, "Simulation of vertical dynamic vehicle–track interaction in a railway crossing using Green's functions," *Journal of Sound and Vibration,* vol. 410, pp. 318-329, 2017.
[8] L. Xin, "Long-Term Behaviour of Railway Crossings Wheel-Rail Interaction and Rail Fatigue Life Prediction," Delft University of Technology, Delft, 2017.
[9] C. D. T. Andersson, "Wheel/rail impacts at a railway turnout crossing," *Proceedings of the Institution of Mechanical Engineers, Part F: Journal of Rail and Rapid Transit,* vol. 212, pp. 123-134, 1998.
[10] E. Kassa, and J. C. O. Nielsen, "Dynamic train–turnout interaction in an extended frequency range using a detailed model of track dynamics," *Journal of Sound and Vibration,* vol. 320, pp. 893-914, 2009.
[11] S. Alfi, F. Braghin, and S. Bruni, "Numerical and experimental evaluation of extreme wheel–rail loads for improved wheelset design," *Vehicle System Dynamics,* vol. 46, pp. 431-444, 2008.
[12] S. Alfi, and S. Bruni, "Mathematical modelling of train–turnout interaction," *Vehicle System Dynamics,* vol. 47, pp. 551-574, 2009.
[13] Y. Q. Sun, C. Cole, and M. McClanachan, "The Calculation of Wheel Impact Force Due to the Interaction between Vehicle and a Turnout," *Proceedings of the Institution of Mechanical Engineers, Part F: Journal of Rail and Rapid Transit,* vol. 224, pp. 391-403, 2010.
[14] E. Kassa, and J. C. O. Nielsen, "Dynamic interaction between train and railway turnout: full-scale field test and validation of simulation models," *Vehicle System Dynamics,* vol. 46, pp. 521-534, 2008.
[15] B. A. Pålsson, and J. C. O. Nielsen, "Wheel–rail interaction and damage in switches and crossings," *Vehicle System Dynamics,* vol. 50, pp. 43-58, 2012.
[16] E. Kassa, and J. C. O. Nielsen, "Stochastic analysis of dynamic interaction between train and railway turnout," *Vehicle System Dynamics,* vol. 46, pp. 429-449, 2008.
[17] C. Wan, and V. L. Markine, "Parametric study of wheel transitions at railway crossings," *Vehicle System Dynamics,* vol. 53, pp. 1876-1901, 2015.
[18] E. Kassa, C. Andersson, and J. C. O. Nielsen, "Simulation of dynamic interaction between train and railway turnout," *Vehicle System Dynamics,* vol. 44, pp. 247-258, 2006.
[19] M. Wiest, E. Kassa, W. Daves, J. C. O. Nielsen, and H. Ossberger, "Assessment of methods for calculating contact pressure in wheel-rail/switch contact," *Wear,* vol. 265, pp. 1439-1445, 2008.
[20] J. Xu, P. Wang, X. Ma, Y. Gao, and R. Chen, "Stiffness Characteristics of High-Speed Railway Turnout and the Effect on the Dynamic Train-Turnout Interaction," *Shock and Vibration,* vol. 2016, pp. 1-14, 2016.
[21] M. Pletz, W. Daves, and H. Ossberger, "A wheel set/crossing model regarding impact, sliding and deformation—Explicit finite element approach," *Wear,* vol. 294-295, pp. 446-456, 2012.
[22] A. Johansson, B. Pålsson, M. Ekh, J. C. O. Nielsen, M. K. A. Ander, J. Brouzoulis, and E. Kassa, "Simulation of wheel–rail contact and damage in switches & crossings," *Wear,* vol. 271, pp. 472-481, 2011.
[23] M. Wiest, W. Daves, F. D. Fischer, and H. Ossberger, "Plastification and Damage in Wheel-Rail Rolling Contact - Case Study on a Crossing," *Pamm,* vol. 5, pp. 67-70, 2005.
[24] M. Pletz, W. Daves, and H. Ossberger, "A wheel passing a crossing nose: Dynamic analysis under high axle loads using finite element modelling*," *Proceedings of the Institution of Mechanical Engineers, Part F: Journal of Rail and Rapid Transit,* vol. 226, pp. 603-611, 2012.

[25] L. Xin, V. L. Markine, and I. Y. Shevtsov, "Numerical analysis of the dynamic interaction between wheel set and turnout crossing using the explicit finite element method," *Vehicle System Dynamics,* vol. 54, pp. 301-327, 2016.
[26] Z. Wei, C. Shen, Z. Li, and R. Dollevoet, "Wheel–Rail Impact at Crossings: Relating Dynamic Frictional Contact to Degradation," *Journal of Computational and Nonlinear Dynamics,* vol. 12, 2017.
[27] Y. Ma, A. A. Mashal, and V. L. Markine, "Modelling and experimental validation of dynamic impact in 1:9 railway crossing panel," *Tribology International,* vol. 118, pp. 208-226, 2018.
[28] W. J. Zwanenburg, "Degradation process of switches and crossings," in The Institution of Engineering and Technology International Conference on Railway Condition Monitoring, Birmingham, UK, 2006.
[29] J. Y. Zhu, and D. J. Thompson, "Characterization of forces, dynamic response, and sound radiation from an articulated switch sleeper in a turnout system," *Proceedings of the Institution of Mechanical Engineers, Part F: Journal of Rail and Rapid Transit,* vol. 224, pp. 53-60, 2009.
[30] D. H. Ossberger, "Modern Turnout Technology for High Speed " Head of Corporate Engineering and R&D VAE GmbH, 2016.
[31] P. Wang, *Design of high-speed railway turnouts: theory and applications*, London: Elsevier, 2015.
[32] R. Chen, J.-y. Chen, P. Wang, J.-m. Xu, and J.-l. Xiao, "Numerical investigation on wheel-turnout rail dynamic interaction excited by wheel diameter difference in high-speed railway," *Journal of Zhejiang University-SCIENCE A,* vol. 18, pp. 660-676, 2017.
[33] R. F. Lagos, A. Alonso, J. Vinolas, and X. Pérez, "Rail vehicle passing through a turnout: analysis of different turnout designs and wheel profiles," *Proceedings of the Institution of Mechanical Engineers, Part F: Journal of Rail and Rapid Transit,* vol. 226, pp. 587-602, 2012.